Available online at www.sciencedirect.com

SciVerse ScienceDirect

Physics Procedia 35 (2012) 134 – 139

Physics Procedia

Positron Studies of Defects 2011

Defect studies of yttria stabilized zirconia with chromia additive

O. Melikhova[a], J. Čížek[a], I. Procházka[a], T.E. Konstantinova[b], I.A. Danilenko[b]

[a]*Charles University in Prague, Faculty of Mathematics and Physics, V Holešovičkách 2, 180 00 Praha 8, Czech Republic*

[b]*Galkin Donetsk Institute for Physics and Engineering, National Academy of Sciences of Ukraine, Luxemburg Street 72, 83114 Donetsk, Ukraine*

Abstract

The effect of chromia (Cr_2O_3) additive on defects in yttria (Y_2O_3) stabilized zirconia (ZrO_2) was examined in the present work. Two kinds of samples were investigated: (i) compacted nanopowders with grain size of 12-23 nm and (ii) sintered ceramics. Defect characterization was performed by high resolution positron lifetime spectroscopy. Because of nanocrystalline grain size positrons in compacted nanopowders probe almost exclusively grain boundaries. It was found that in compacted nanopowders positrons are trapped in vacancy-like misfit defect at grain boundaries and in larger defects situated at triple points. On the other hand, in ceramics positrons are annihilated predominantly in Zr-vacancies in grain interiors. Our results give a strong evidence for segregation of Cr cations at grain boundaries. Positron lifetime results for compacted nanopowders are strongly influenced by the Cr_2O_3 concentration, while results obtained in ceramics are very similar independently on the Cr_2O_3 content. Moreover, it was found that Cr_2O_3 additive completely suppresses the formation of positronium in open inter-granular volumes.

PACS: number(s): 78.70.Bj, 61.46.Hk, 81.07.Wx

Keywords: yttria stabilized zirconia; nanocrystaline materials; ceramics

1. Introduction

Zirconium dioxide (ZrO_2, zirconia) takes considerable attention as engineering material because of high melting point of 2700°C, low electronic as well as thermal conductivities and favorable mechanical properties (enhanced strength and fracture toughness) [1]. Three zirconia polymorphs are known to exist at the ambient pressure [1]. A high temperature cubic phase is stable at temperatures above 1380°C. At lower temperatures zirconia transforms into a tetragonal phase and subsequently below 1200°C into a monoclinic phase. Large volume changes occurring during phase transition into the low temperature monoclinic phase lead to undesired crack formation and the material falls into pieces. The high temperature zirconia phases (cubic or tetragonal) can be stabilized down to room temperature

* Corresponding author: Tel.: +420221912788; Fax: +420221912567; E-mail address: Oksana.Melikhova@mff.cuni.cz.

1875-3892
doi:10.1016/j.phpro.2012.06.024

by addition of suitable oversized cations [1]. Yttria (Y_2O_3) containing Y^{3+} cations is used most frequently for stabilization. Such system is then called yttria stabilized zirconia (YSZ). An addition of 3-8 mol.% of yttria is sufficient to stabilize the tetragonal zirconia phase down to room temperature (so called partially stabilized YSZ). When yttria content exceeds 8 mol. % the high temperature cubic zirconia phase is stabilized (so called fully stabilized YSZ). Currently, there is a growing interest in ternary systems of YSZ doped with other cations which provide an additional degree of freedom in tailoring of material properties. Chromium is an interesting dopant due to its multivalence and smaller ionic radius with respect to zirconium.

Previous investigations [2-4] of YSZ clearly demonstrated that positron annihilation spectroscopy (PAS) provides valuable information about structure of grain boundaries, point defects and residual porosity in YSZ nanocrystalline materials and ceramics. In the present work PAS was employed for structural investigations of partially stabilized YSZ doped with chromia (Cr_2O_3).

2. Experimental

Partially stabilized YSZ nanopowders doped with chromia were prepared by co-precipitation technique [5] using water solutions of $ZrO(NO_3)_2$, $Y(NO_3)_3$ and $Cr(NO_3)_3$ mixed at stoichiometric ratios. Precipitates were dried at 120°C and calcinated at 600°C for 2 h on air. Calcinated nanopowders were subsequently compacted into disk shaped pellets (diameter ≈ 10 mm, thickness ≈ 5 mm) by a uniaxial pressure of 500 MPa. These samples are referred in the following text as 'compacted nanopowders'. In addition, ceramic samples were prepared from compacted nanopowders by sintering at 1350°C for 2h. The compacted nanopowders and ceramic samples of the following compositions were investigated: ZrO_2 + 3%mol. Y_2O_3 + x mol. % Cr_2O_3, where x = 0, 0.3, 0.7, 1.5, 2.9, 5.0.

To investigate exclusively the effect of chromia doping a binary ZrO_2 + 3%mol. Cr_2O_3 compacted nanopowder was prepared. In addition, tetragonal ZrO_2 + 3%mol Y_2O_3 single crystal and monoclinic pure zirconia compacted nanopowder were investigated as reference samples.

A carrier-free $^{22}Na_2CO_3$ positron source (≈ 1.3 MBq) sealed between 2 μm thick mylar foils was used for PAS measurements. Positron lifetime (LT) measurements were performed on a digital spectrometer described in Ref. [6]. The spectrometer is equipped with BaF_2 scintillators and fast photomultipliers Hamamatsu H3378 and exhibits an excellent time resolution of 145 ps (FWHM ^{22}Na). Detector pulses were digitized using a couple of 8-bit ultra-fast digitizers Acqiris DC 211 with sampling frequency of 4 GHz and stored in a PC. Analysis of sampled waveforms and construction of LT spectrum was performed off-line using so called integral true constant fraction technique described in Ref. [7]. LT spectra, which always contained at least 10^7 positron annihilation events, were decomposed using a maximum likelihood based procedure [8]. The source contribution consisted of two weak components with lifetimes of ~368 ps and ~1.5 ns and corresponding intensities of ~6 % and ~1 %.

3. Results and discussion

3.1. Compacted nanopowders

Results of LT measurements for compacted nanopowders (i.e. lifetimes τ_i and relative intensities I_i of the exponential components resolved in LT spectra) are listed in Tables 1 and 2. One can see in Table 1 that LT spectra of all compacted nanopowders studied here contain two components originating from annihilation of positrons. The calculated bulk lifetime τ_B for the tetragonal zirconia phase falls in the interval 141-150 ps depending on the approach used in calculation [4]. Since lifetimes of the both components resolved in LT spectra are significantly longer than τ_B they can be attributed to positrons trapped in defects. Hence, compacted nanopowders contain a high density of defects which leads to saturated positron trapping. This is not surprising since X-ray diffraction studies revealed that compacted nanopowders exhibit nanocrystalline grains with size of 12-23 nm [4,9] which is smaller than positron diffusion length L_+ in oxides, e.g. L_+ = 52 nm was measured in ZnO single-crystal [10]. Hence, in compacted nanopowders virtually all positrons thermallized inside grains diffuse to grain boundaries and are trapped in open volume defects there. Theoretical calculations performed in Ref. [4] clearly showed that O-vacancies as well as their possible complexes with Y cations are too shallow traps incapable of positron localization. On the other hand, Zr vacancy is a deep positron trap. The shorter component with lifetime τ_1 represents, therefore, a contribution of positrons trapped in open volume misfit defects with size comparable to Zr-vacancy located at grain boundaries. It is known that grain boundaries in an ionic crystal may carry an electric potential resulting from the presence of the

excess ions of one sign [11]. It was found that grain interfaces in YSZ are positively charged due to segregation of yttrium [12,13]. This potential is compensated by a negatively charged compensating layer adjacent to grain boundaries and characterized by depletion of positively charged O-vacancies [14]. Although positively charged regions in general repulses positrons, in case of grain boundaries in YSZ the size of the potential barrier is just a few tenths of eV [11,14], which does not prevent positrons from getting trapped in deep potential wells like vacancy-like misfit defects at grain interfaces.

Table 1 Lifetimes τ_i and relative intensities I_i of the exponential components resolved in LT spectra of pure ZrO_2 compacted nanopowder, binary ZrO_2+ 3mol.%Y_2O_3 and ZrO_2+ 3mol.% Cr_2O_3 compacted nanopowders and ternary ZrO_2+ 3mol.%Y_2O_3 + x mol. % Cr_2O_3 compacted nanopowders and ceramics. First two columns show yttria and chromia concentration expressed in mol. %. The quantity τ_f calculated using Eq. (2) in order to check the consistency of decomposition with the three state simple trapping model (when applicable) is shown in the table as well. The last column provides information whether a Ps contribution was detected in LT spectrum or not. Parameters of Ps components are listed in Table 2.

Y_2O_3 (mol. %)	Cr_2O_3 (mol. %)	τ_1 (ps)	I_1 (%)	τ_2 (ps)	I_2 (%)	τ_3 (ps)	I_3 (%)	τ_f (ps)	Ps
Compacted nanopowders									
-	-	-	-	188(3)	43(2)	374(4)	46(2)	-	Yes
3.0	-	-	-	178(3)	28(2)	374(3)	61(2)	-	Yes
-	3.0	-	-	196(5)	15.6(8)	385(1)	84.4(8)	-	No
3.0	0.3	-	-	191(3)	31.4(9)	381(2)	68.6(9)	-	No
3.0	0.7	-	-	191(3)	26.0(8)	390(2)	74.0(8)	-	No
3.0	2.9	-	-	209(2)	20(1)	398(5)	80(1)	-	No
3.0	5.0	-	-	260(10)	20(1)	393(4)	80(2)	-	No
Ceramics									
3.0	-	40(10)	5(2)	176(2)	88(1)	322(9)	7.2(6)	156(5)	No
3.0	0.3	36(9)	4(1)	176(4)	91(1)	357(9)	5.0(5)	156(5)	No
3.0	0.7	35(9)	6(2)	176.7(8)	90(2)	380(10)	4.0(5)	145(5)	No
3.0	1.5	40(10)	4(1)	176(1)	91.6(5)	363(9)	4.4(2)	157(5)	No
3.0	2.9	40(10)	5(3)	176.8(9)	89(3)	380(9)	5.7(2)	153(5)	No

Table 2 Lifetimes $\tau_{o\text{-}Ps,i}$ and relative intensities $I_{o\text{-}Ps,i}$ of the long-lived exponential components representing a contribution of o-Ps pick-off annihilation which were resolved in LT spectra of compacted nanopowders without chromia. In fitting of LT spectra a p-Ps contribution with lifetime of $\tau_{p\text{-}Ps}$ = 125 ps and relative intensity $I_{p\text{-}Ps} = 1/3(I_{o\text{-}Ps,1} + I_{o\text{-}Ps,2})$ was assumed. The components originating from annihilation of positrons are given in Table 1.

Y_2O_3 (mol. %)	Cr_2O_3 (mol. %)	$\tau_{o\text{-}ps,1}$ (ns)	$I_{o\text{-}Ps,1}$ (%)	$\tau_{o\text{-}ps,2}$ (ns)	$I_{o\text{-}Ps,2}$ (%)
-	-	1.9(1)	1.9(1)	31(2)	6.0(3)
3.0	-	1.8(1)	1.5(1)	30(2)	6.1(3)

The longer component with lifetime τ_2 represents a contribution of positrons trapped in larger point defects (vacancy clusters) with open volume comparable with a few monovacancies. These defects are situated in intersections of two or more grain boundaries (triple points).

One can see in Table 1 that pure ZrO_2 compacted nanopowder exhibits lifetime $\tau_2 \approx 188$ ps. Binary compacted nanopowder ZrO_2 + 3 mol.% Y_2O_3 exhibits slightly shorter lifetime $\tau_2 \approx 178$ ps while the sample ZrO_2 + 3 mol.% Cr_2O_3 exhibits slightly longer lifetime $\tau_2 \approx 196$ ps. Hence segregation of Cr at grain boundaries seems to slightly increase the size of vacancy like open volume misfit defects at grain interfaces. This is most probably due to smaller ionic radius of Cr compared to Zr. Interestingly, ternary compacted nanopowders exhibit also prolonged lifetime τ_2 which is comparable with that measured in ZrO_2 + 3 mol.% Cr_2O_3 sample. Moreover, τ_2 increases with increasing chromia content, see Table 1. This testifies a strong segregation of Cr cations at grain boundaries since in compacted nanopowders positrons annihilate almost exclusively at grain interfaces [4]. It was found that Cr cations increase the binding energy of OH groups with surface of nanoparticles resulting in the inhibition of hydroxide/oxide transformation and thereby an increase of the crystallization temperature [9]. This is consistent with our results and supports the picture that Cr cations segregate at the surface of YSZ nanoparticles.

Grain boundary is an areal defect with two macroscopic dimensions. Hence, the volume density of grain boundaries is proportional to the inverse of the grain size d. Assuming a uniform distribution of vacancy-like misfit defects along grain boundaries, the concentration c_V of these defects is also proportional to the inverse of the grain size, $c_V \sim d^{-1}$. On the other hand, vacancy clusters at triple points are point defects. In the case of uniform grain

size, there is a constant number of such vacancy clusters per grain. Thus, the volume concentration c_T of vacancy clusters at triple points is proportional to the number of grains in the unit volume, $c_T \sim d^{-3}$, for detailed discussion see Ref. [4]. Due to saturated positron trapping at defects occurring in the studied compacted nanopowders, the ratio of relative intensities I_3 and I_2 equals to the ratio of positron trapping rates to corresponding defects

$$\frac{I_3}{I_2} = \frac{\nu_T c_T}{\nu_V c_V} = k^2 \frac{1}{d^2}, \quad (1)$$

where ν_T and ν_V are the specific positron trapping rate to vacancy clusters at triple points and to vacancy-like defects, respectively, and k is a material dependent constant. Fig. 1 shows dependence of I_3/I_2 ratio on d^{-2} for ternary ZrO_2 + 3%mol. Y_2O_3 + x mol. % Cr_2O_3 compacted nanopowders. The grain size d for compacted nanopowders was determined by XRD in Ref. [7]. The results obtained on binary YSZ compacted nanopowders in Ref. [4] are also shown in the figure for comparison. One can see in the figure that the dependence of I_3/I_2 ratio on d^{-2} can be reasonably approximated by a linear relationship described by Eq. (1). The proportionality constant k = (24 ± 2) nm obtained from a linear regression of all data in Fig. 1 is in good agreement with that determined for binary YSZ compacted nanopowders in Ref. [4].

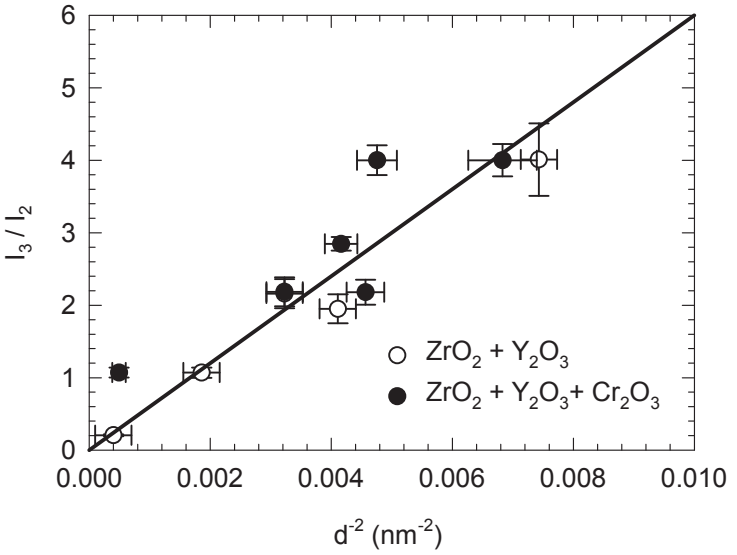

Figure 1 Ratio I_3/I_2 plotted against the inverse square of the particle size d for the ternary compacted nanopowders ZrO_2 + 3 mol.% Y_2O_3 + x mol.% Cr_2O_3 (full points). Data for binary compacted nanopowders ZrO_2 + x mol.% Y_2O_3 studied in Ref. [4] are also plotted in the figure by open points for comparison.

In addition to the components originating from positron annihilation a positronium (Ps) contribution was found in LT spectra of ZrO_2 and ZrO_2 + 3%mol. Y_2O_3 compacted nanopowders, i.e. samples without chromia. Two long-lived components with lifetimes $\tau_{o\text{-}Ps,1}$, $\tau_{o\text{-}Ps,2}$ and relative intensities $I_{o\text{-}Ps,1}$, $I_{o\text{-}Ps,2}$ which come from the pick-up annihilation of ortho-positronium (o-Ps) are given in Table 2. The principal o-Ps component $\tau_{o\text{-}Ps,2} \approx 30$ ns corresponds to mesopores with diameter of ≈ 3 nm estimated on the basis of the semi-empirical correlation between the o-Ps pick-off lifetime and the cavity size [15]. Since compacted nanopowders usually contain some residual porosity the principal o-Ps component can be attributed to o-Ps localized in big cavities between crystallites. The shorter and weaker o-Ps component with lifetime $\tau_{o\text{-}Ps,1} \approx 1.9$ ns can be attributed to smaller voids with diameter ≈ 0.6 nm estimated using the Tao-Eldrup model [14,15]. These sub-nanometer voids are probably situated at intersections of crystallite interfaces.

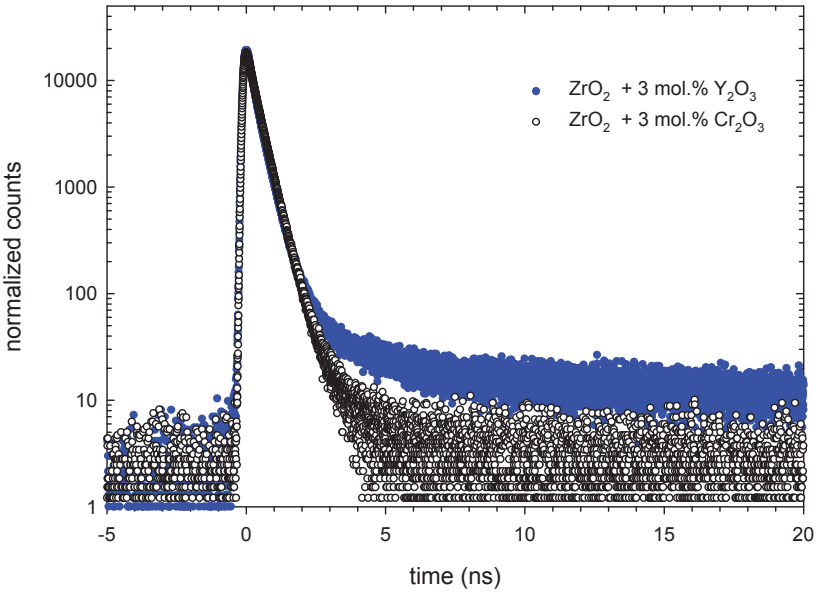

Figure 2 Normalized LT spectra measured on ZrO_2 + 3 mol.% Cr_2O_3 (full points) and ZrO_2 + 3 mol.% Y_2O_3 (full points).

No Ps contribution was detected in the compacted nanopowders containing chromia. Even an addition of only x = 0.3 mol. % of Cr_2O_3 is sufficient to suppress Ps contribution in compacted nanopowders below the detection limit (I_{o-Ps} < 0.5 %). This distinctive effect of Cr_2O_3 addition can be seen in Fig. 2 where normalized LT spectra with subtracted background are compared. The long-lived o-Ps contribution is clearly visible in case of ZrO_2 + 3mol.% Y_2O_3 sample but is absent in ZrO_2 + 3mol.% Cr_2O_3 compacted nanopowder. X-ray photoelectron spectroscopy (XPS) revealed that in ternary ZrO_2 + 3%mol. Y_2O_3 + x mol. % Cr_2O_3 nanopowders yttrium ions are present in the main oxide state Y^{3+} only. On the other hand, chromium ions are present not only in the main oxidation state of chromia Cr^{3+}, but also in Cr^{2+} and Cr^{5+} oxide states. The paramagnetic Cr^{5+} ions act as donors and introduce electrons into grain boundaries. As a consequence any bound state between a positron and an electron localized at grain boundary is immediately broken in collisions with these quasi-free electrons introduced by Cr^{5+} ions. Since Ps can be localized only in open volumes among particles suppression of the Ps component by chromia doping testifies a strong segregation of Cr ions at grain boundaries.

3.2. Ceramics

Lifetimes and relative intensities of exponential components resolved in LT spectra of ceramic samples are listed in Table 1. Contrary to nanocrystalline compacts the results obtained for all ceramic samples are very similar independently on the chromia content. All ceramics exhibit three-component LT spectrum. The shortest component with lifetime $\tau_1 < \tau_B$ represents obviously contribution of free positrons, while the second component with lifetime $\tau_2 \approx 176$ ps and dominating intensity $I_2 \approx 90\%$ comes from positrons trapped in vacancy-like point defects and the longest component with lifetime τ_3 can be attributed to positrons trapped in vacancy clusters. Since the free positron component was resolved in LT spectra one can check whether the decomposition is consistent with the three state simple trapping model (STM) [16]. If STM assumptions, i.e. uniform spatial distribution of defects, no trapping of non-thermalized positrons and no detrapping, are fulfilled then the quantity

$$\tau_f = \left(\sum_i \frac{I_i}{\tau_i} \right)^{-1} \tag{2}$$

equals the bulk positron lifetime τ_B. One can see in Table 1 that the quantity τ_f calculated using Eq. (2) is in a satisfactorily agreement with the tetragonal zirconia bulk lifetime taking into account relatively large uncertainty of τ_f due to low intensity of the free positron component and also spread of τ_B values obtained from the theory.

TEM observations [4] confirmed that sintering at high temperatures leads to a substantial grain growth which is reflected by a strong decrease of I_3/I_2 ratio. Hence, in contrast to compacted nanopowders, positrons in ceramic samples are annihilated predominantly in grain interiors because the volume fraction of grain boundaries was drastically reduced. This is supported also by the lifetime of the dominating component in ceramic samples $\tau_2 \approx 176$ ps, which is shorter than lifetime measured in compacted nanopowders but agrees well with the single component lifetime of (175 ± 1) ps for YSZ single crystals [4]. This testifies that positrons in ceramic samples annihilates in Zr-vacancies in grain interiors. Due to this reason LT results for ternary ceramic samples are basically independent on the chromia content since positrons are not influenced by Cr cations located predominantly at grain boundaries.

4. Conclusions

Partially stabilized YSZ compacted nanopowders and ceramics doped with chromia were prepared and characterized. In compacted nanopowders positrons probe almost exclusively grain boundaries due to nanocrystalline grain size, while in ceramics positrons are annihilated predominately in grain interiors. In nanocrystalline compacts PAS results are strongly influenced by chromia content, while in all ceramics we obtained very similar results independently on the chromia concentration. This testifies a strong segregation of Cr cations at grain boundaries. Moreover, electrons introduced into grain boundaries by Cr^{5+} cations completely suppress the formation of positronium at inter-granular open volumes.

Acknowledgements

This work was supported by the Czech Academy of Science (KJB101120906), the Czech Science Foundation (P108/11/1396) and the Ministry of Schools, Youths and Sports of the Czech Republic (MSM 0021620834).

References

[1] A.H. Heuer, L.W. Hobbs in: Science and Technology of Zirconia. Advances in Ceramics, vol. 3. (The American Ceramic Society, Columbus, OH, 1981).
[2] K. Ito, Y. Yagi, S. Hirano, M. Miyayama, T. Kudo, A. Kishimoto, and Y. Ujihira, J. Ceram. Soc. Jpn. 107 (1999) 123.
[3] J. E. Garay, S. C. Glade, P. Asoka-Kumar, U. Anselmi-Tamburini, and Z. A. Munir, J. Appl. Phys. 99 (2006) 024313.
[4] J. Čížek, O. Melikhova, I. Procházka, J. Kuriplach, R. Kužel, G. Brauer, W. Anwand, T. E. Konstantinova, I. A. Danilenko, Phys. Rev. B 81 (2010) 024116.
[5] A.M. Korduban, I.A. Yashschishyn, T E. Konstantinova, I.A. Danilenko, G.K. Volkova, V.A. Glazunova, Functional Materials 14, (2007) 454.
[6] F. Bečvář, J. Čížek, I. Procházka, J. Janotová, J. Nucl Instrum Methods A 539 (2005) 372.
[7] F. Bečvář, Nucl Instrum Methods B 261 (2007) 871.
[8] I. Procházka, I. Novotný, F. Bečvář, Mater. Sci. Forum 255-257 (1997) 772.
[9] I.A. Yashschishyn, A.M. Korduban, V.V. Trachevskiy, T.E. Konstantinova, I.A. Danilenko, G.K. Volkova, I.K. Nosolev, Functional Materials 17 (2010) 306.
[10] T. Koida, S. F. Chichibu, A. Uedono, A. Tsukazaki, M. Kawasaki, T. Sota, Y. Segawa, H. Koinuma, Appl. Phys. Lett. 82 (2003) 532.
[11] W.D. Kingery, J. Am. Ceram. Soc. 57 (1974) 1.
[12] X. Guo, R. Waser, Prog. Mater. Sci. 51 (2006) 151.
[13] X. Guo, Solid State Ionics 81 (1995) 235.
[14] X. Guo, Z. Zhang, Acta Mater. 51 (2003) 2539.
[15] K. Ito, H. Nakanishi, and Y. Ujihira, J. Phys. Chem. B 103 (1999) 4555.
[14] M. Eldrup, D. Lightbody, and J. Sherwood, J. Chem. Phys. 63 (1981) 51.
[15] S. Tao, J. Chem. Phys. 56 (1972) 5499.
[16] R. West, in Positrons in Solids, edited by P. Hautojärvi (Springer-Verlag, Berlin, 1979), p. 89.